

An experimental and numerical study on long-term deformation of SRC columns

Gyeong-Hee An^{1a}, Jun-Ki Seo^{2b}, Sang-Lyul Cha^{1c} and Jin-Keun Kim^{*1}

¹Department of Civil and Environmental Engineering, Korea Advanced Institute of Science and Technology,
291 Daehak-ro, Yuseong-gu, Daejeon 34141, Republic of Korea

²Construction & Environment Team, Gyeongin Construction Headquarters, Korea Electric Power Corporation,
140 Toegy-ro, Jung-gu, Seoul 04629, Republic of Korea

(Received January 31, 2017, Revised July 24, 2018, Accepted August 3, 2018)

Abstract. Long-term deformation of a steel-reinforced concrete (SRC) column is different from that of a reinforced concrete (RC) column due to the different moisture distribution. Wide-flange steel in an SRC column obstructs diffusion and makes long-term deformation slower. Previous studies analyzed the characteristics of long-term deformation of SRC columns. In this study, an additional experiment is conducted to more precisely investigate the effect of wide-flange steel on the long-term deformation of SRC columns. Long-term deformation, especially creep of SRC columns with various types of wide-flange steel, is tested. Wide-flange steel for the experiment is made of thin acrylic panels that can block diffusion but does not have strength, because the main purpose of this study is to exclusively demonstrate the long-term deformation of concrete caused by moisture diffusion, not by the reinforcement ratio. Experimental results show that the long-term deformation of a SRC column develops slower than that in a RC column, and it is slower as the wide-flange steel hinders diffusion more. These experimental results can be used for analytical prediction of long-term deformation of various SRC columns. An example of the analytical prediction is provided. According to the experimental and analytical results, it is clear that a new prediction model for long-term deformation of SRC columns should be developed in further studies.

Keywords: long-term deformation; creep; shrinkage; steel-reinforced concrete; column shortening; moisture diffusion

1. Introduction

Steel-reinforced concrete (SRC) columns are frequently used for high-rise buildings because of the increased load-bearing capacity and construction convenience. Prediction of the column shortening in high-rise buildings is much more important than in low-rise buildings because a small error can create problems with the safety of structures as well as their serviceability.

Previous research showed that the long-term deformation of the SRC column is different from that of the RC column due to different moisture diffusion (Seol *et al.* 2008, An *et al.* 2015). In this study, an additional experiment is conducted to more precisely investigate the effect of wide-flange steel on the long-term deformation of SRC columns. Unlike the previous experiment, thin acrylic panels are used for the wide-flange steel to exclusively simulate the effect of wide-flange steel and exclude the effect of the reinforcement ratio on the moisture diffusion

and long-term deformation. Further, the type of wide-flange steel becomes more diverse than in previous experiments. Details about the experiment are shown in this paper.

In comparison with the previous experiment, experimental results in this research clearly show that the long-term deformation of SRC columns develops slower than RC columns and it is resulted from the slower moisture diffusion in concrete, not from the reinforcement ratio because acrylic wide-flange steel hardly affect the mechanical properties of columns. Additionally, the effect of the type of wide-flange steel is experimentally shown in this research.

Long-term deformation of SRC columns can also be predicted in an analytical way that calculates the shrinkage strain from the change in relative humidity inside the concrete. Analytical prediction is compared with the experimental results, and analytical parameters related to the diffusion and shrinkage can be determined through the comparison. Prediction of other kinds of SRC columns is also possible based on the analytical parameters determined in this experiment. Analysis is useful for prediction of certain types of columns used in the field. An example of the analytical prediction is included in this paper.

2. Experimental program

The purpose of the experiment is to compare the long-term deformation, especially creep of RC and SRC

*Corresponding author, Professor
E-mail: kimjinkeun@kaist.ac.kr

^aPh.D.
E-mail: akh425@kaist.ac.kr

^bAssociate
E-mail: jkseo17@kepco.co.kr

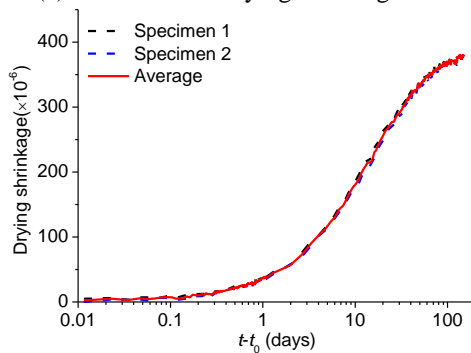
^cPh.D.
E-mail: maikuraki@kaist.ac.kr

Table 1 Mix proportion of concrete

W/C	S/a	Unit weight (kg/m ³)				
		W	C	S	G	SP
0.45	0.43	170	378	754	1008	2.27



(a) Picture of the drying shrinkage test



(b) Experimental result

Fig. 1 Experiment for the drying shrinkage of concrete

columns, caused by the different kinds of moisture diffusion. Four types of columns are made and the creep of each column is tested. The reinforcement ratio in all the columns is set to zero to exclude the effect of the reinforcement ratio and only consider the long-term deformation of the concrete. Therefore, thin acrylic panels are used to simulate the wide-flange steel in the SRC column. Fundamental material properties, such as the compressive strength, elastic modulus, and drying shrinkage of concrete, are also tested in accordance with the Korean Industrial Standards (KS). Details of the material properties and the creep test setup of columns are as follows.

2.1 Materials

2.1.1 Concrete

Mixture

Table 1 gives the mix proportion of concrete for the research. Ordinary Portland Cement (OPC) is used. *W*, *C*, *S*, *G*, and *SP* in Table 1 stand for water, cement, sand, gravel, and superplasticizer, respectively. The specific gravity of the fine aggregate and the coarse aggregate are 2.55 and 2.58, and the fineness modulus of the fine aggregate and the coarse aggregate are 2.6 and 6.25, respectively. The maximum size of the coarse aggregate is 13 mm.

Compressive strength and elastic modulus

Cylindrical specimens for the tests of compressive

Table 2 Experimental results of compressive strength (MPa)

Age(days)	7	14	28
Specimen			
1	34.1	37.5	45.9
2	36.8	42.2	44.6
3	32.8	41.0	41.3
4		40.1	
5		41.8	
6		39.0	
Average	34.6	40.3	43.9
Standard deviation	1.67	1.63	1.94

Table 3 Experimental results of elastic modulus (GPa)

Age(days)	7	14	28
Specimen			
1	22.6	25.5	24.9
2	23.5	25.0	26.7
3	23.2	26.0	27.9
4		25.3	
5		25.0	
Average	23.1	25.3	26.5
Standard deviation	0.38	0.37	1.24

strength and elastic modulus of concrete are made in accordance with the standard, KS F 2403(2014) corresponding to ASTM C192 (2016). Specimens are also tested in accordance with the standard, KS F 2405 (2010) corresponding to ASTM C39 (2016) at the age of 7, 14, and 28 days. For specimens with the age of 7 and 28 days, three specimens with a size of $\phi 100 \times 200$ mm are prepared. Creep experiment of all column specimens started at the age of 14 days, therefore, three additional specimens are tested for 14 days and the size of the specimen is decided as $\phi 150 \times 300$ mm which is more similar to the size of column specimens to reduce the effect of size on compressive strength. Specimens are cured under water at 20 °C. Experimental results of the mechanical properties of concrete used for the column specimens are shown in Table 2 and Table 3.

Drying shrinkage

Drying shrinkage is tested in accordance with the standard, KS F 2424 (2015) corresponding to ASTM C157 (2014). Specimens are rectangular with a size of $100 \times 100 \times 400$ mm, and embedment strain gauges (Model: EGP5-120) are installed in the middle of the specimens. Two identical specimens are used for the test, and they are cured under water at 20 °C for 14 days. The specimens are exposed to a temperature of 20 °C and relative humidity of 60% after 14 days of curing. During the drying shrinkage test, both ends of the specimens are sealed with foil tape as shown in Fig. 1(a). The specimens can be considered as an infinitely long specimen by sealing the ends. This sealing blocks diffusion at both ends, and diffusion can be considered as a two dimensional problem. The specimens are placed on top of rollers for free shrinkage. The experimental results of the drying shrinkage are shown in Fig. 1(b).

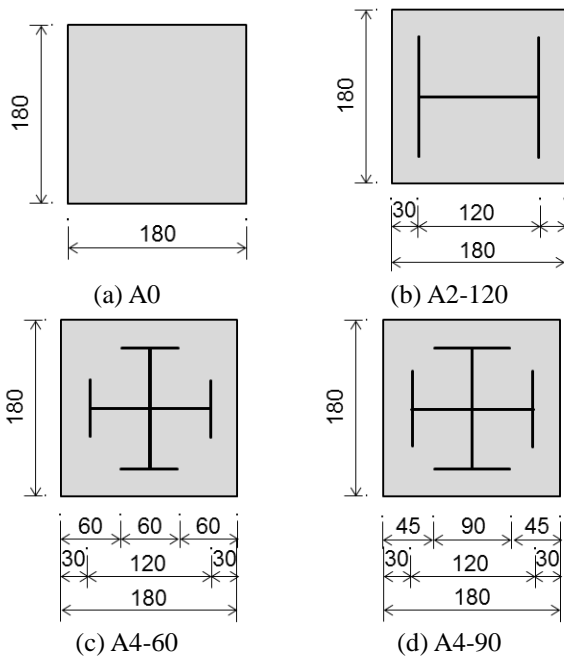


Fig. 2 Cross-sections of SRC columns experimented

2.1.2 Wide-flange steel

Thin acrylic panels with thickness about 0.5 mm are used instead of the actual wide-flange steel in the SRC columns. This acrylic panel obstructs the moisture diffusion but does not affect the strength of the specimen. Therefore, the experimental result only reflects the change in moisture diffusion due to the acrylic panel.

2.2 Creep of columns

2.2.1 Specimens

Four types of columns and two identical specimens for each type of column are made for the creep experiment. The width and depth of all the columns are 180 mm and the total height is 500 mm. A larger column would be better for the experiment, but unfortunately, the capacity of a hydraulic jack to exert pressure on the column and the dimensions of the test frame are not sufficient for a larger specimen. The size is the maximum size for the available test equipment.

Fig. 2 shows the cross-section types of the specimens according to the shape of the wide-flange steel. One type called 'A0' is for RC column, and it does not contain any acrylic panels so the moisture freely diffused. The others, namely 'A2-120', 'A4-60' and 'A4-90', are for the SRC columns, and they contain the acrylic panels with various lengths as shown in Fig. 2. The columns are classified for the shape of the acrylic panel. 'A2-120' means that two acrylic panels that are the flange parts of the wide-flange steel in Fig. 2(b) affect the moisture diffusion and the lengths of the panels are 120 mm. 'A4-60' means that four acrylic panels affect the diffusion and the lengths of panels are 60 mm.

The height of the acrylic panel is 480 mm, and it is fixed by thin wires to the four walls of molds as shown in Fig. 3. An embedded strain gauge (Model: EGP5-120) is set in the column specimens at the center as shown in Fig. 3.



Fig. 3 Installation of acrylic panels and embedded strain gauge (Top view, A4-90)



Fig. 4 Test setup for creep of the columns

Concrete is placed in a longitudinal direction to produce a uniform cross-section of the column. The surfaces of the top and bottom of the columns need to be flat to avoid stress concentration during the creep test. Therefore, cement paste is placed at the top of the columns to make the surfaces smooth before removing the molds. The water-cement ratio for the cement paste is chosen as 0.25 to have more strength than the column specimen to prevent destruction of the paste due to the loading. Cement paste about 10 mm thick is applied to the top surface of all the specimens and hardened for four hours. After removing the molds, the column specimens are cured in water of 20°C for 14 days. The top and bottom surfaces of the specimens are sealed with foil tape as shown in the shrinkage specimens after curing before the creep test starts.

2.2.2 Test method

The test method is basically the same as for a normal creep test. Loading is applied at the age of 14 days and the loading level is about 20% of the compressive strength at the age of 14 days. The temperature and relative humidity around the specimens are 20°C and 52%. There are two specimens for each type of column, and the two specimens are tested together under the same frame. Creep is observed for about 200 days after loading.

Fig. 4 shows the final test setup for creep of the columns. Two linear variable differential transformers (LVDT) are additionally set for one specimen of each type as shown in Fig. 4 to check the measurement from embedded gauge.

3. Analytical program

Numerous studies suggest the theoretical backgrounds and analytical programs for analyzing the moisture

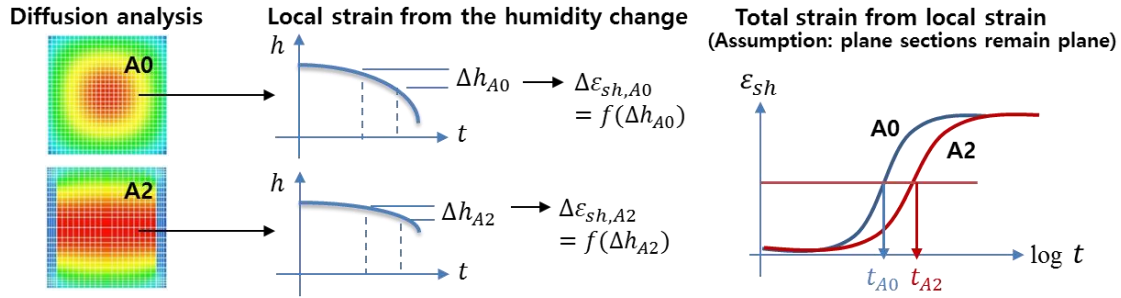


Fig. 5 Schematic explanation of the analytical program

diffusion and long-term deformation of concrete. Among them, theories and programs used for this research are shown as follow.

3.1 Structure of program

The program mainly consists of two parts, moisture diffusion analysis (Bažant and Najjar 1972, Ba *et al.* 2014, Zhang *et al.* 2015, Patel *et al.* 2016) and the stress and strain analysis (Bažant and Xi 1994, Abbasnia *et al.* 2009, Azenha *et al.* 2011, Idiart *et al.* 2011). Finite element method is used for the program. The 8-node hexaheron solid element is employed and the size of mesh is from 7 to 15 mm. Galerkin method and Crank-Nicolson method which are common methods for numerical solution of partial differential equations such as diffusion. Moisture distribution is analyzed based on the diffusion model and the result is expressed as the relative humidity in concrete. The total stress and strain of a column can be calculated from the humidity change by the diffusion analysis. A schematic explanation of the analytical program is shown in Fig. 5. Models and conditions for the program are the same as in previous studies (Kim and Lee 1998, Seol *et al.* 2008, An *et al.* 2015). Thus, four important parameters in the program rather than the entire program are introduced in this paper.

3.2 Four parameters for the analysis

The first parameter is the diffusion coefficient D which relates to the speed of diffusion inside the concrete. Several types of diffusion coefficients are suggested by various researchers (Bažant and Thonguthai 1978, Mihashi and Numao 1989, Akita *et al.* 1990, Chari *et al.* 2016). Eq. (1) shows one of the diffusion coefficients for the isotherm condition suggested in *fib* 2010 (Federation Internationale du Beton (*fib*) 2013).

$$D(h) = D_1 \left(\alpha + \frac{1-\alpha}{1 + [(1-h)/(1-h_c)]^n} \right) \quad (1)$$

where h is the pore relative humidity, D_1 is the maximum moisture diffusion coefficient when $h=1.0$, α is the ratio of the maximum D to minimum D , h_c is the pore relative humidity at $D=0.5D_1$ and n is an exponent.

The second parameter is the surface factor f which is essential for the boundary condition of the diffusion analysis defined as Eq. (2) (Sakata 1983).

$$D \left(\frac{\partial h}{\partial n} \right)_s = f(h_{en} - h_s) \quad (2)$$

where h_{en} is the ambient relative humidity, h_s is the surface relative humidity, and n is the unit outward normal at the surface.

The last two parameters are the ultimate free shrinkage ε_s^o and the constant for shrinkage r which are used for calculating the drying shrinkage and drying creep as Eq. (3) (Bažant and Xi 1994).

$$\Delta \varepsilon_{sh} = \varepsilon_s^o \frac{E_c(t_\infty)}{E_c(t)} (1 + r\sigma_c) \Delta f_s(h) \quad (3)$$

where ε_{sh} is shrinkage and stress-induced shrinkage which is known as drying creep, E_c is the Young's modulus of concrete, σ_c is the stress of concrete, t_∞ is the ultimate time of drying, and $f_s(h)=1-h^3$.

Total creep of concrete is sum of basic creep and drying creep, therefore, a basic creep model is also necessary to analyze the long-term deformation in addition to the drying creep suggested in Eq. (3). There are basic creep models in the B3 model (Bažant and Baweja 1995) and *fib* 2010 model (Federation Internationale du Beton (*fib*) 2013). The B3 model is used for the basic creep analysis in this study.

4. Results and discussion

4.1 Discussion on the experimental results

The parameters used for the analysis of SRC columns are determined by comparing the analytical results with the experimental results of drying shrinkage and creep of the 'A0' column. It is appropriate to find the parameters from those experimental results because the parameters are related to the material properties, and both shrinkage specimens and 'A0' specimens are made of concrete only. Table 4 shows the ranges of the parameters suggested in the literature and the optimized parameters based on the experimental results of drying shrinkage and creep of the 'A0' column. The optimized values in Table 4 are found by trial and error method based on the suggested range. Optimized parameters are reasonable as shown in Table 4, and these optimized parameters are used for the creep analysis of SRC columns experimented.

Table 4 Parameters for analysis

Parameter	Suggested range in literature	Optimized value for this research
D_1	$4.17 \times 10^{-7} - 1.67 \times 10^{-6}$ *	1.11×10^{-6}
D	h_c	0.75
(m^2/h)	n	7
	α	0.05
f (m/h)	1.2×10^{-4} **	1.1×10^{-4}
ϵ_s^o	$5.0 \times 10^{-4} - 5.0 \times 10^{-3}$ ***	5.1×10^{-4}
r	$7.25 \times 10^{-3} - 7.25 \times 10^{-2}$ ***	1.85×10^{-1}
		(Embedded gauge) 2.1×10^{-1} (LVDT)

* (Bažant and Najjar 1972)

** $f = 2.17 \times 10^{-3}(w/c) - 8.56 \times 10^{-4}$ (Sakata 1983)

*** (Bažant and Xi 1994)

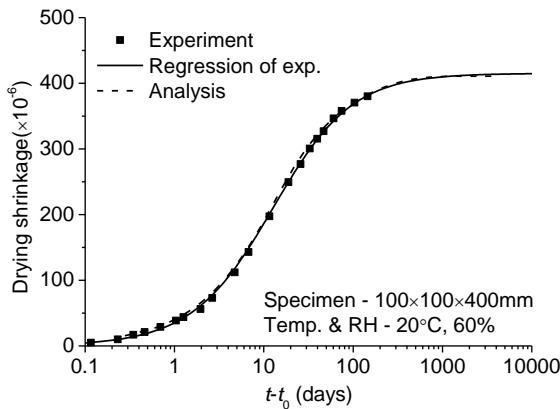
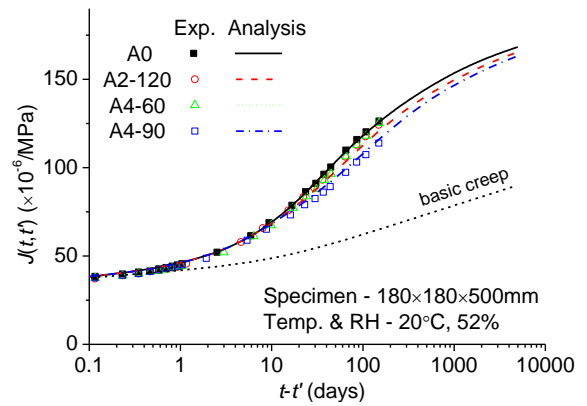


Fig. 6 Comparison of the experiment and the analysis of drying shrinkage specimen

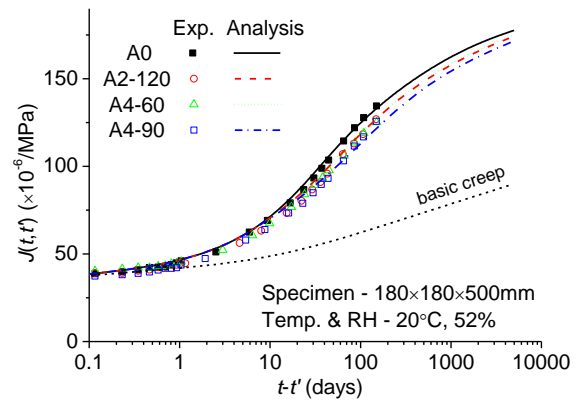
Fig. 6 shows the comparison of the analysis using the parameters in Table 4 and the experiment of the drying shrinkage. Fig. 7 also shows the comparison of the analyses from the parameters in Table 4 and the experiments of creep for various columns. Fig. 7(a) and Fig. 7(b) show the results from the embedded strain gauge and LVDT, respectively. Basic creep is assumed by B3 model for the analysis as shown in Fig. 7.

As shown in Fig. 6 and Fig. 7, drying shrinkage and the creep of the ‘A0’ column show good agreement between measurements and analyses. Therefore, the analytical parameters in Table 4 are reasonable for analyzing the creep of the other SRC columns. Once the analytical parameters are determined as in Table 4, the long-term deformation of the SRC columns can be analyzed by FEM with the same parameters but different cross sections. The analytical results of ‘A2-120’, ‘A4-60’, and ‘A4-90’ through this process are shown in Fig. 7.

Creep in the SRC columns (A2-120, A4-60, A4-90) is developed more slowly than in the RC column (A0) depending on the type of wide-flange steel inside the column as shown in Fig. 7. From the results in Fig. 7, it is concluded that, as expected, the creep in the SRC column is affected more when the wide-flange steel disturbs the moisture diffusion more. Additionally, creep in ‘A2-120’



(a) Embedded strain gauge



(b) LVDT

Fig. 7 Comparison of the experiments and the analyses of creep of various columns

and ‘A4-60’ is similar because the length of the wide-flange steel affecting the moisture diffusion is the same. Although there is a small difference between the embedded strain gauge and LVDT, the tendency is similar in both sensors.

4.2 Prediction of long-term deformation of SRC columns

The column for the experiment is not large enough to observe a significant difference but the size is the maximum for the available test equipment, as explained in the section 2.2.1. However, the long-term behavior of columns which are made of same concrete but have larger sizes than the experiment can be analytically predicted. This prediction for the large SRC columns from the small ones experimented is quite reasonable because the analytical parameters are optimized based on the experimental results and it means that the parameters consider the material properties of concrete.

For example, the long-term deformation of the 1000x1000 mm columns in Fig. 8 can be predicted by using the same parameters in Table 4 if the concrete is assumed to be the same as the concrete used for the experiment. ‘A0-L’ in Fig. 8(a) is the same type of ‘A0’ in Fig. 2(a) with the larger size. Similar to Fig. 2, ‘A2-900’ and ‘A4-675’ represent the number and the length of the acrylic panels. A type of column, ‘A4-450’, is not analyzed because it is similar to the type ‘A2-900’ as explained.

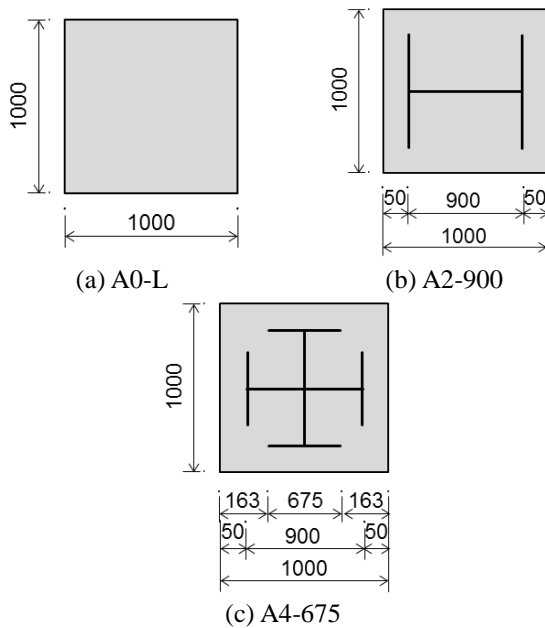


Fig. 8 Cross-sections for the analysis of large SRC columns

Predicted drying shrinkage and creep of columns are shown in Fig. 9(a) and Fig. 9(b).

The difference between the RC and SRC columns is more significant in Fig. 9 compared to Fig. 7 because the size of the columns and the proportion of the wide-flange steel are bigger. Drying shrinkage is more affected by the wide-flange steel than creep as shown in Fig. 9. For example, time taken by ‘A2-900’ to reach the strain of 200×10^{-6} in drying shrinkage is about 2400 days and it is about twice the time taken by ‘A0-L’ column as marked in Fig. 9(a).

Prediction graphs of SRC columns in Fig. 9 are horizontally shifted and a bit tilted compared to RC column. In addition, the RC and SRC columns experience the same deformation until a certain age, and then start to show a difference. Therefore, it is concluded that the effect of wide-flange steel is not the same as the effect of a size increase of the column.

5. Conclusions

Conclusions of this research are as follows.

- Experiments for long-term deformation of various SRC columns are conducted to investigate the effect of wide-flange steel compared to RC columns. Creep of three types of SRC columns are tested. The material for the simulation of wide-flange steel is chosen as the acrylic panel to isolate the effect of wide-flange steel on moisture diffusion.
- Experimental results show that the long-term deformation of SRC columns is delayed compared to RC columns due to the delayed moisture diffusion caused by wide-flange steel. Therefore, the long-term deformation of SRC columns depends on the type of wide-flange steel.
- Experimental results show good agreement with the

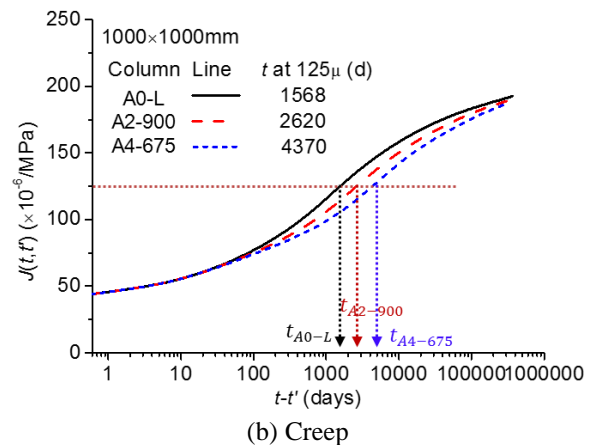
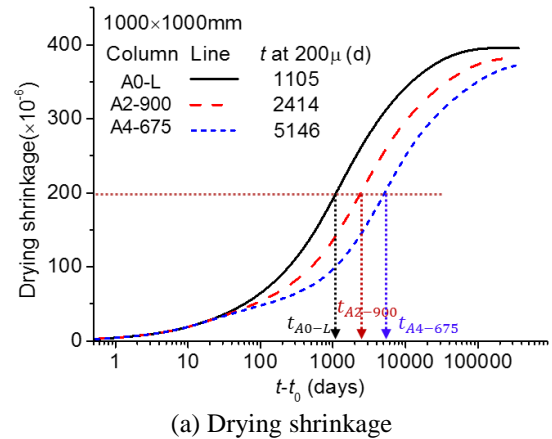


Fig. 9 Prediction of long-term deformation of columns with 1000×1000 mm sections

analytical results. Analytical parameters for the experiment can be used for the analysis for other types of columns. In other words, long-term deformation of large size columns can be analyzed from experiments with small columns.

- Some correction coefficients for the current creep model are necessary to reflect the characteristics of SRC columns and give better prediction for SRC columns. Analytical study on the long-term deformation of various SRC columns with respect to column size or environmental conditions will be the subject of further research to develop appropriate correction factors.

Acknowledgments

This work was supported by a Mid-career Researcher Program grant through the NRF funded by the MEST of the Korean government (NRF-2016R1A2B4016394).

References

- Abbasnia, R., Kanzadi, M., Zadeh, M.S. and Ahmadi, J. (2009), ‘Prediction of free shrinkage strain related to internal moisture loss’, *Int. J. Civil Eng.*, **7**(2), 92-98.
- Akita, H., Fujiwara, T. and Ozaka, Y. (1990), ‘Water movement within mortar due to drying and wetting’, *Proceeding of JSCE*,

- 420, 61-69. (in Japanese)
- An, G.H., Kwon, S.H. and Kim, J.K. (2015), "Effect of wide-flange-steel geometry on the long-term shortening of steel-reinforced concrete columns", *Mag. Concrete Res.*, **67**(23), 1242-1256.
- ASTM C157 (2014), Standard Test Method for Length Change of Hardened Hydraulic-cement Mortar and Concrete, American Society for Testing Materials; West Conshohocken, PA, USA.
- ASTM C192 (2016), Standard Practice for Making and Curing Concrete Test Specimens in the Laboratory, American Society for Testing Materials, West Conshohocken, PA, USA.
- ASTM C39 (2016), Standard Test Method for Compressive Strength of Cylindrical Concrete Specimens, American Society for Testing Materials, West Conshohocken, PA, USA.
- Azenha, M., Sousa, C., Faria, R. and Neves, A. (2011), "Thermo-hygro-mechanical modelling of self-induced stresses during the service life of RC structures", *Eng. Struct.*, **33**(12), 3442-3453.
- Ba, M.F., Qian, C.X. and Gao, G.B. (2014), "Nonlinear calculation of moisture transport in underground concrete", *Comput. Concrete*, **13**(3), 361-375.
- Bazant, Z.P. and Baweja, S. (1995), "Creep and shrinkage prediction model for analysis and design of concrete structures-model B3", *Mater. Struct.*, **28**(6), 357-365.
- Bazant, Z.P. and Najjar, L.J. (1972), "Nonlinear water diffusion in nonsaturated concrete", *Mater. Struct.*, **5**(1), 3-20.
- Bazant, Z.P. and Thonguthai, W. (1978), "Pore pressure and drying of concrete at high temperature", *J. Eng. Mech.*, ASCE, **104**(EM5), 1059-1079.
- Bazant, Z.P. and Xi, Y. (1994), "Drying creep of concrete: constitutive model and new experiments separating its mechanisms", *Mater. Struct.*, **27**(1), 3-14.
- Chari, M.N., Shekarchi, M., Ghods, P. and Moradian, M. (2016), "A simple practical method for determination of moisture transfer coefficient of mature concrete using a combined experimental-numerical approach", *Comput. Concrete*, **18**(3), 367-388.
- Federation Internationale du Beton (*fib*) (2013), *fib Model Code for Concrete Structures 2010*, Ernst&Sohn.
- Idiart, A., Lopez, C. and Carol, I. (2011), "Modeling of drying shrinkage of concrete specimens at the meso-level", *Mater. Struct.*, **44**(2), 415-435.
- Kim, J.K. and Lee, C.S. (1998) "Prediction of differential drying shrinkage in concrete", *Cement Concrete Res.*, **28**(7), 985-994.
- KS F 2403 (2014), Standard Test Method for Making and Curing Concrete Specimens, Korean Industrial Standards, Seoul, Republic of Korea.
- KS F 2405 (2010), Standard Test Method for Compressive Strength of Concrete, Korean Industrial Standards, Seoul, Republic of Korea.
- KS F 2424 (2015), Standard Test Method for Length Change of Mortar and Concrete, Korean Industrial Standards, Seoul, Republic of Korea.
- Mihashi, H. and Numao, T. (1989), "Influence of curing condition on a diffusion process of concrete at elevated temperatures", *Proc. JPN Concrete Inst.*, **11**(1), 229-234.
- Patel, R., Phung, Q., Steetharam, S., Perko, J., Jacques, D., Maes, N., Schutter, G., Ye, G. and Breugel, K. (2016), "Diffusivity of saturated ordinary Portland cement-based materials: A critical review of experimental and analytical modelling approaches", *Cement Concrete Res.*, **90**, 52-72.
- Sakata, K. (1983), "A study on moisture diffusion in drying and drying shrinkage of concrete", *Cement Concrete Res.*, **13**(2), 216-224.
- Seol, H.C., Kwon, S.H., Yang, J.K. and Kim, J.K. (2008), "Effect of differential moisture distribution on the shortening of steel-reinforced concrete columns", *Mag. Concrete Res.*, **60**(5), 313-322.
- Zhang, W., Tong, F., Gu, X. and Xi, Y. (2015), "Study on moisture transport in concrete in atmospheric environment", *Comput. Concrete*, **16**(5), 775-793.

CC